

Lawrence Berkeley National Laboratory

Computational Research

Title

Bose-Einstein correlations of same-sign charged pions in the forward region in pp collisions at $\sqrt{s}=7$ TeV

Permalink

<https://escholarship.org/uc/item/18f2t0g5>

Journal

Journal of High Energy Physics, 2017(12)

ISSN

1126-6708

Authors

The LHCb collaboration

Aaij, R

Adeva, B

et al.

Publication Date

2017-12-01

DOI

10.1007/jhep12(2017)025

Peer reviewed

RECEIVED: September 7, 2017

REVISED: November 15, 2017

ACCEPTED: November 28, 2017

PUBLISHED: December 6, 2017

Bose-Einstein correlations of same-sign charged pions in the forward region in pp collisions at $\sqrt{s} = 7$ TeV



The LHCb collaboration

E-mail: Marcin.Kucharczyk@cern.ch

ABSTRACT: Bose-Einstein correlations of same-sign charged pions, produced in proton-proton collisions at a 7 TeV centre-of-mass energy, are studied using a data sample collected by the LHCb experiment. The signature for Bose-Einstein correlations is observed in the form of an enhancement of pairs of like-sign charged pions with small four-momentum difference squared. The charged-particle multiplicity dependence of the Bose-Einstein correlation parameters describing the correlation strength and the size of the emitting source is investigated, determining both the correlation radius and the chaoticity parameter. The measured correlation radius is found to increase as a function of increasing charged-particle multiplicity, while the chaoticity parameter is seen to decrease.

KEYWORDS: Hadron-Hadron scattering (experiments), Particle correlations and fluctuations, QCD

ARXIV EPRINT: [1709.01769](https://arxiv.org/abs/1709.01769)

Contents

1	Introduction	1
2	BEC measurement	2
2.1	Two-particle correlation function	2
2.2	Reference sample	3
2.3	Double ratio	3
2.4	Coulomb correction	3
3	Detector and dataset	4
4	Selection and model fitting	5
5	Systematic uncertainties	7
6	Results	9
7	Summary and conclusions	12
	The LHCb collaboration	17

1 Introduction

Multiparticle production within the process of hadronisation can be investigated by measuring Bose-Einstein correlations (BEC) between indistinguishable bosons [1, 2]. The technique to study the BEC effect in particle physics is the analogue of the Hanbury-Brown-Twiss (HBT) intensity interferometry [3–5]. The production of identical bosons that are close in phase space is enhanced by the presence of BEC. The measurements of the quantum interference effect between indistinguishable particles emitted by a finite-size source are useful to understand the space-time properties of the hadron emission volume.

Since the first observation of BEC in identically charged pions produced in $p\bar{p}$ collisions [6], the effect has been studied for multiboson systems produced in leptonic, hadronic and nuclear collisions [7–32]. At the LHC, the BEC effect has been studied by the ALICE, ATLAS and CMS collaborations in proton-proton [26–30], proton-lead [31] and lead-lead [31, 32] collisions.

Dependences of the BEC effect upon various observables have been studied, including charged-particle multiplicity, average transverse momentum of the particle pair and boson mass. The latter has been reported by the LEP experiments [7–21], and can be interpreted within some theoretical models [33–36].

In this paper, the first study of the BEC effect in pp collisions in the forward region is presented. The BEC parameters characterising the correlation radius and the chaoticity of the correlation source are measured.

2 BEC measurement

Quantum interference effects are probed by studying the Lorentz invariant quantity Q [2, 37] of two indistinguishable particles of rest mass m and four-momenta q_1 and q_2

$$Q = \sqrt{-(q_1 - q_2)^2} = \sqrt{M^2 - 4m^2}, \quad (2.1)$$

which gives a measure of the phase-space separation of the two-particle system of invariant mass M .

2.1 Two-particle correlation function

The BEC effect is expected to manifest itself as an enhancement in the two-particle correlation function in the low- Q region below $\sim 0.5 \text{ GeV}/c^2$, expressed as [38]

$$C_2(Q) = \frac{\rho_2(Q)}{\rho_2^0(Q)}, \quad (2.2)$$

where $\rho_2(Q)$ is the two-particle density function for like-sign pairs of indistinguishable particles, as defined in ref. [38], and $\rho_2^0(Q)$ is the corresponding density function without the BEC effect, which is constructed as described in section 2.2. The densities $\rho_2(Q)$ and $\rho_2^0(Q)$ are normalised to unity, such that they can be interpreted as probability density functions. The correlation function $C_2(Q)$ is commonly parameterised as a Fourier transform of the source density distribution, $C_2(Q) = N(1 + \lambda e^{-|RQ|^{\alpha_L}})$ [39], where the parameter R , the correlation radius, can be interpreted as the radius of the spherically symmetric source of the emission volume, N accounts for the overall normalisation and λ is the chaoticity parameter, which accounts for the partial incoherence of the source [40]. The chaoticity parameter can vary from zero, in the case of a completely coherent source, to unity for an entirely chaotic source. The Levy index of stability [39], α_L , accounts for the assumed density distribution. The radial distribution of the static source corresponding to the case of $\alpha_L = 1$ is used in the present analysis

$$C_2(Q) = N(1 + \lambda e^{-RQ}) \times (1 + \delta \cdot Q), \quad (2.3)$$

where the δ parameter accounts for long-range correlations, e.g. related to the transverse momentum conservation. This extended parameterisation follows better the Q distribution in data, including in the low- Q region below $\sim 0.5 \text{ GeV}/c^2$ [41].

The correlation function is, to first order, independent of the single-particle acceptance and efficiency. By construction of the correlation function, the effects due to the detector occupancy, acceptance and material budget are accounted for by dividing the Q distribution for like-sign pion pairs by a reference distribution.

2.2 Reference sample

The reference sample used to construct the $\rho_2^0(Q)$ density function, present in the denominator of eq. (2.2), should reflect the distribution without the BEC effect while maintaining all other correlations. A number of reference samples can be constructed but none fully satisfies the above conditions. The reference sample may be constructed using experimental data, or with simulated events incorporating the detector interactions.

A data-driven “event-mixed” reference sample [42] is used in the present analysis. This approach is based on the choice of two identical bosons, each originating from different events, which naturally do not contain the BEC effect. However, this method of constructing boson pairs may not contain other correlations present in the same-sign boson data sample, such as correlations due to Coulomb interactions or long-range effects.

Alternative methods have been considered for constructing the reference sample. For example, the reference sample could consist of opposite-sign charged bosons originating from the same pp interaction. As in the event-mixed reference sample, the main advantage of the opposite-sign approach is that the reference distribution is derived directly from data. However, the opposite-sign charge pairs may also originate from resonances which result in local enhancements in the Q spectrum. Furthermore, correlations arising from the attraction of opposite charges are present in such a sample. Another method is to employ the simulated Q distribution without the BEC effect. In this case, the crucial requirement is a good level of agreement between data and simulated samples in the distributions of crucial variables, e.g. the particle momenta. The absence of the Coulomb and spin effects in generators based on the Lund Model [43] may impinge on the correctness of this method.

2.3 Double ratio

To account for imperfections in the reference distribution derived from the data a “double ratio” r_d is commonly used in BEC studies

$$r_d(Q) \equiv \frac{C_2(Q)^{\text{data}}}{C_2(Q)^{\text{simulation}}}, \tag{2.4}$$

where $C_2(Q)^{\text{data}}$ denotes the correlation function in the data constructed using the event-mixed reference sample, while $C_2(Q)^{\text{simulation}}$ indicates the correlation function in the simulation without the BEC effect, using an event-mixed sample built with simulated events in the same way as for data. The correlation function in the simulation without the BEC effect includes the simulated long-range correlations that are also present in data. Therefore, if the long-range correlations are correctly modelled, a constant $r_d(Q)$ distribution is expected in the high- Q region up to $\sim 2.0 \text{ GeV}/c^2$. In the present analysis the BEC effect is measured by fitting the $r_d(Q)$ distribution with the event-mixed reference sample, using the parameterisation given in eq. (2.3).

2.4 Coulomb correction

Final-state interactions involving both electromagnetic (Coulomb) and strong forces are present in the low- Q region below $\sim 0.5 \text{ GeV}/c^2$, and may potentially affect the distributions

of the analysed observables. In the low- Q region, the Coulomb repulsion between two identically charged hadrons alters the correlation function $C_2(Q)$ by decreasing the BEC effect. This effect is corrected for with the Gamov penetration factor [44, 45], $G_2(Q)$, by applying a weight per particle pair $1/G_2(Q)$, where $G_2(Q) = \frac{2\pi\zeta}{e^{2\pi\zeta}-1}$, $\zeta = \pm \frac{\alpha m}{Q}$, and m and α denote the particle rest mass and the fine-structure constant, respectively. The sign of ζ is positive for same-charge and negative for opposite-charge pairs of hadrons.

The Coulomb interactions are not present in the simulated samples used in the analysis. This effect therefore has to be corrected for in the data.

3 Detector and dataset

The LHCb detector [46] is a single-arm forward spectrometer designed for the study of particles containing b or c quarks. The detector includes a high-precision tracking system consisting of a silicon-strip vertex detector (VELO) [47] surrounding the pp interaction region and covering the pseudorapidity range $2 < \eta < 5$, a large-area silicon-strip detector located upstream of a dipole magnet with a bending power of about 4 Tm, and three stations of silicon-strip detectors and straw drift tubes [48] placed downstream of the magnet. The tracking system provides a measurement of momentum, p , with a relative uncertainty that varies from 0.5% at low momentum to 1% at 200 GeV/ c . The minimum distance of a track to a primary vertex (PV), the impact parameter (IP), is measured with a resolution of $(15 + 29/p_T) \mu\text{m}$, where p_T is the component of p transverse to the beam, in GeV/ c . Different types of charged hadrons are distinguished using information from two ring-imaging Cherenkov detectors [49]. Photon, electron and hadron candidates are identified by a calorimeter system consisting of scintillating-pad and preshower detectors, an electromagnetic calorimeter and a hadronic calorimeter. Muons are identified by a system composed of alternating layers of iron and multiwire proportional chambers [50]. The trigger [51] consists of a hardware stage, based on information from the calorimeter and muon systems, followed by a software stage, which applies a full event reconstruction.

In the present analysis, a dataset of no-bias and minimum-bias triggered events collected in 2011 at a centre-of-mass energy of $\sqrt{s} = 7$ TeV is used. The no-bias trigger selects events randomly, while the minimum-bias trigger requires at least one reconstructed VELO track. The data were collected with an average number of visible interactions per bunch crossing¹ (pile-up) of 1.4 [52]. In order to eliminate biases related to the trigger requirements, a sample of “independent pp interactions” is constructed as described in section 4.

In the simulation, pp collisions are generated using PYTHIA 8 [53] with a specific LHCb configuration [54] and without including the BEC effect. Decays of hadronic particles are described by EVTGEN [55], in which final-state radiation is generated using PHOTOS [56]. The interaction of the generated particles with the detector and its response are implemented using the GEANT4 toolkit [57, 58], as described in ref. [59]. To study systematic effects, an additional sample is simulated using PYTHIA 6.4 [60] with the Perugia0 [61] tune.

¹A visible interaction corresponds to the PV reconstructed with at least five VELO tracks.

4 Selection and model fitting

The analysis uses a sample of events that may contain multiple pp collisions. In the absence of trigger requirements each pp interaction in the event can be analysed separately. Therefore, if the event is selected by the no-bias trigger, all PVs are accepted. In the case of events with multiple pp collisions selected by the minimum-bias trigger, the related biases are suppressed by randomly removing one of the PVs containing the track(s) on which the trigger is fired.

The correlation function is constructed using pairs of same-sign pions. The particle identification (PID) is based on the output of a neural network employing subdetector information that quantifies the probability for a particle to be of a certain kind [62]. Such probabilities are calibrated to account for differences between data and the simulation that is used to train the neural network. The corrected values are derived from the data distributions using dedicated PID calibration samples [49]. A high purity of the pion sample has to be ensured, but without suppressing low-momentum pions which mostly contribute to the signal region at low Q . The optimal limit on the pion identification probability is applied at the point where the signal enhancement in the low- Q region below $\sim 0.5 \text{ GeV}/c^2$ for data begins to saturate. The pion purity with this selection remains high ($\sim 98\%$). Additional vetoes on the kaon and proton identification probabilities are also imposed.

The following single particle requirements are applied. The selection requires that all pion candidates must have reconstructed track segments in the VELO, with $2 < \eta < 5$, and tracking stations downstream of the magnet. Each track must have a good-quality track fit, $p_T > 0.1 \text{ GeV}/c$, and no associated signal in the muon stations. Both pion candidates must be assigned to the same PV. Particles are assigned to the PV for which the χ^2 value of the impact parameter, χ_{IP}^2 , is the smallest, where χ_{IP}^2 is defined as the difference in the vertex-fit χ^2 of a given PV reconstructed with and without the track under consideration. A loose requirement on the track IP, $\text{IP} < 0.4 \text{ mm}$, is applied to retain most of the particles originating from a given PV. In order to reduce the contamination from fake and clone tracks,² in the case where the tracks have all the same hits deposited in the VELO subdetector, only the track with the best χ^2 is retained. In addition, fake tracks are removed using the requirements on the track χ^2 and the output of a dedicated neural network [62].

In the region $Q < 0.05 \text{ GeV}/c^2$, the separation in momentum between two particles is degraded and is not well simulated. The discrepancy between data and simulated track pairs tends to increase as Q approaches zero. Investigations using simulation indicate that there is a significant fraction of pion pairs containing fake and clone tracks in the region $Q < 0.05 \text{ GeV}/c^2$ for all activity classes. The double ratio is approximately constant and close to unity in the high- Q region up to $Q \sim 2.0 \text{ GeV}/c^2$ (see figure 2), which indicates that the long-range correlations are modelled accurately in this region. Consequently, the fits to the r_d distributions are restricted to the range $0.05 < Q < 2.0 \text{ GeV}/c^2$.

²Fake tracks are wrongly reconstructed tracks which combine the hits deposited by multiple particles in the tracking detectors. Clone tracks are two or more tracks reconstructed by mistake from the hits deposited in detectors by a single particle.

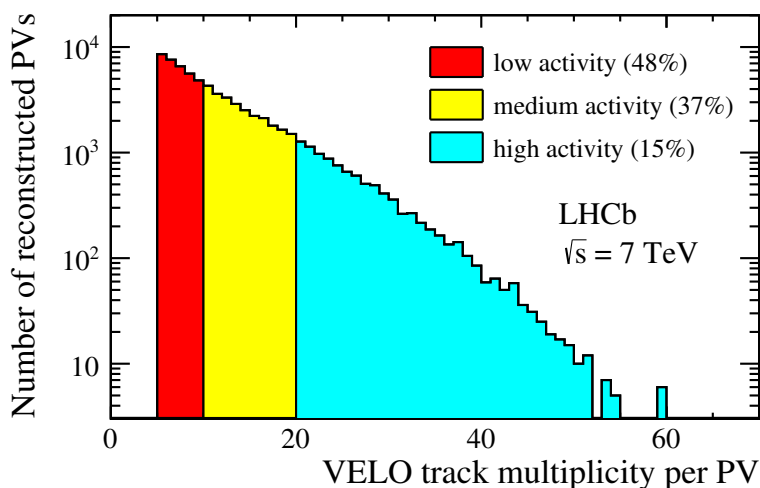


Figure 1. Multiplicity of reconstructed VELO tracks assigned to a PV for the 2011 no-bias sample. Different colours indicate three activity classes defined as fractions of the full distribution. The minimum value of the track multiplicity to accept reconstructed PV is five.

The BEC effect is expected to be largest in the low- Q region below $\sim 0.5 \text{ GeV}/c^2$, where it may be affected by same-sign clone tracks. Such clone pion pairs should manifest themselves as an enhancement in the distribution of the differences of the tangents of the track momenta of the two particles, where the tangents are measured in the xz and yz planes before the magnet, with the z axis defined along the beam direction. The tangents are used to estimate the number of clone tracks remaining after the final selection, and the clone tracks can be suppressed with a requirement on the difference between the tangents of the two particles in a pair. Pion pairs are removed from the analysis if both $|\Delta t_x|$ and $|\Delta t_y|$ are less than 0.3 mrad, where Δt_x and Δt_y are the differences of the tangents of the track momenta of the two particles in the xz and yz planes. After applying these requirements, the effect of the clone particles is found to be negligible in the region $Q > 0.05 \text{ GeV}/c^2$.

The BEC parameters are studied as a function of the charged-particle multiplicity. However, the measured charged-particle multiplicities cannot be directly used to compare results among different experiments, mainly because the detector acceptances may not overlap and the reconstruction efficiencies may differ. This is why activity classes are introduced, reflecting the total multiplicity in the full solid angle. Three activity classes are defined in the range $2 < \eta < 5$ according to the multiplicity of reconstructed VELO tracks assigned to a PV, which is a good probe of the total multiplicity. These activity classes are illustrated in figure 1. The *low activity class* corresponds to a fraction of 48% of PVs with lowest multiplicities (from 5 to 10 tracks). The *medium activity class* contains the 37% of PVs with higher multiplicities (from 11 to 20 tracks). Finally, the *high activity class* contains 15% of the highest multiplicity PVs (≥ 21 tracks). Using this classification, the comparison among different experiments is largely independent from specific features of the detectors.

Although the activity classes have advantages in comparing results among various experiments characterised by different rapidity ranges, an unfolding procedure is performed to relate the reconstructed charged-particle multiplicities to those predicted by PYTHIA 8 with a specific LHCb configuration [54]. The multiplicity distributions are corrected using a Bayesian unfolding technique [63]. An unfolding matrix reflecting the probability of reconstructing a certain number of charged particles from a single PV in the range $2 < \eta < 5$ with generated charged-particle multiplicity N_{ch} is populated using simulation and applied to the data. It is found that the corrected multiplicities agree well with the unfolded multiplicities previously determined by LHCb in ref. [64]. The activity classes correspond to the following generated charged-particle multiplicity intervals: $N_{ch} \in [8, 18]$ (low activity), $N_{ch} \in [19, 35]$ (medium activity) and $N_{ch} \in [36, 96]$ (high activity).

The distributions of the double ratio of correlation functions in data and simulation for like-sign pion pairs, determined using the event-mixed reference sample, are fitted in the range $0.05 < Q < 2.0 \text{ GeV}/c^2$ for the three different activity classes using the parameterisation of eq. (2.3). The results of the binned maximum likelihood fit to the double ratio are summarised in section 6.

5 Systematic uncertainties

The properties of the correlation function and the construction of the double ratio make the fitted BEC parameters insensitive to the choice of the selection requirements to a large extent. However, due to imperfections in the reference sample and possible differences between data and simulation related to the generation model, as well as subtle reconstruction effects (like the reconstruction of close tracks sharing the same VELO hits or the track reconstruction in the high-occupancy detector regions), some second-order distortions in the double ratio may appear. The systematic uncertainties on the fit parameters, R and λ , of the exponential model are determined by performing the analysis with modifications designed to estimate the systematic effects on individual contributions to the $r_d(Q)$ distribution.

The leading source of systematic uncertainty is due to differences in the event generators used to determine the correlation function for the simulation. To study this effect, a sample of minimum-bias events produced using the PYTHIA 6.4 generator with Perugia0 tuning is used to construct the double ratio. The corresponding contribution to the systematic uncertainty is taken as the difference between the central values of the results obtained using the PYTHIA 8 and PYTHIA 6.4 datasets.

Another important source of systematic uncertainty is related to the PV multiplicity in the event. The constructed double ratio may be distorted in events containing multiple PVs, due to imperfections in the construction of the reference sample. To estimate the associated systematic uncertainty, the sample is divided into three subsamples containing events with one, two, and three or more PVs. For each subsample, the fit is performed and the maximum difference for each measured parameter is taken as a systematic uncertainty. The systematic uncertainty resulting from the PV reconstruction efficiency is also considered. To account for the effect of pile-up in the data and inefficiencies in the PV reconstruction,

a systematic uncertainty is estimated as the difference between the nominal fit results and the results obtained from a fit to the data in which the PV reconstruction has been repeated after removing randomly a subset of the tracks from the event.

After applying the track quality requirements, the fraction of remaining fake tracks is determined from simulation to be at the level of 1%. To determine the systematic uncertainty due to the presence of such fake tracks, the double ratio is refitted with looser track quality requirements. A similar uncertainty is obtained from a second method in which sets of randomly selected uncorrelated tracks are added. The observed change in BEC parameters is negligible with respect to the statistical uncertainty.

The fraction of like-sign pion pairs containing a clone track after the selection is determined to be below 1%. The systematic uncertainty due to the presence of clone tracks is estimated by fitting the double ratio $r_d(Q)$, after applying a tight requirement on the Kullback-Leibler distance [65] such that the clone contribution is fully removed in simulation. The effect is found to be negligible for all activity classes.

The systematic uncertainty due to the calibration of the particle identification in the simulation is estimated by comparing several variants of the calibration procedure with the acceptance evaluated in different binning schemes for the particle momentum, pseudorapidity and track multiplicity. The largest difference after refitting the double ratios is taken as a systematic uncertainty.

As the requirement on the pion identification probability alters the contamination of pions due to misidentification, it can influence the values of the R and λ parameters. The contribution of this effect to the systematic uncertainty is estimated by refitting $r_d(Q)$ with the requirement on the pion identification probability changed to increase the fraction of misidentified pions by 50%.

The systematic uncertainty derived from the fit range in the low- Q (high- Q) region is determined by changing the lower (upper) limit of the Q value by $\pm 0.01 \text{ GeV}/c^2$ ($\pm 0.2 \text{ GeV}/c^2$). The fits to the double ratio with two different lower (upper) limits of Q are performed for the three activity classes and the largest difference is taken as a systematic uncertainty.

The systematic uncertainty due to Coulomb corrections is estimated by varying the corrections by $\pm 20\%$. The variation in the fit parameters is found to be less than 0.1%, and is therefore neglected. It is also found that imposing different requirements on the particle IPs has no significant influence on the measured correlation radius or chaoticity parameter. The fractions of kaon-kaon and proton-proton like-sign pairs misidentified as a pion pair in the pion sample in the BEC signal region of $Q < 1.0 \text{ GeV}/c^2$ are found to be negligible. Pairings of different particle types have a negligible effect.

Other effects like the fit binning, the resolution of the Q variable, different magnet polarities, beam-gas interactions and residual acceptance effects related to possible differences between data and simulation in the low- Q region below $\sim 0.2 \text{ GeV}/c^2$, are also studied and found to be negligible.

The contributions to the systematic uncertainty are listed in table 1. Correlations of the systematic uncertainties between different activity classes are negligible.

Source	Low activity		Medium activity		High activity	
	ΔR [%]	$\Delta\lambda$ [%]	ΔR [%]	$\Delta\lambda$ [%]	ΔR [%]	$\Delta\lambda$ [%]
Generator tunings	6.6	4.3	8.9	3.5	6.5	1.5
PV multiplicity	5.9	5.8	6.1	4.5	3.9	4.3
PV reconstruction	1.8	0.1	1.4	1.2	0.1	<0.1
Fake tracks	0.4	1.1	1.7	3.9	1.1	0.8
PID calibration	1.3	0.3	0.8	0.6	2.7	0.9
Requirement on pion PID	2.9	1.8	1.6	0.1	1.3	0.1
Fit range at low- Q	1.2	1.0	1.2	1.5	1.8	2.7
Fit range at high- Q	1.8	0.1	2.1	0.8	2.4	1.4
Total	9.8	7.6	11.4	7.3	8.8	5.6

Table 1. Fractional systematic uncertainties on the R and λ parameters for the three activity classes, as described in the text. The total uncertainty is the sum in quadrature of the individual contributions.

Activity	N_{ch}	R [fm]	λ	δ [GeV $^{-1}$]
Low	[8,18]	$1.01 \pm 0.01 \pm 0.10$	$0.72 \pm 0.01 \pm 0.05$	$0.089 \pm 0.002 \pm 0.044$
Medium	[19,35]	$1.48 \pm 0.02 \pm 0.17$	$0.63 \pm 0.01 \pm 0.05$	$0.049 \pm 0.001 \pm 0.009$
High	[36,96]	$1.80 \pm 0.03 \pm 0.16$	$0.57 \pm 0.01 \pm 0.03$	$0.026 \pm 0.001 \pm 0.010$

Table 2. Results of fits to the double ratio $r_d(Q)$ for the three different activity classes and corresponding N_{ch} bins, using the parameterisation of eq. (2.3). Statistical and systematic uncertainties are given separately.

6 Results

The results of fits to the double ratios for the correlation radius, chaoticity parameter and δ parameter for the three different activity classes are summarised in table 2, including statistical and systematic uncertainties, and are presented in figure 2.

The dependences of the correlation radius and the chaoticity parameter on the activity class are shown in figures 3 and 4, respectively. As the activity class increases, the R parameter also increases, while the λ parameter decreases. This confirms previous observations at LEP [19] and in the other LHC experiments [26, 28–30]. There are no theoretical predictions for the BEC effect in pp interactions, however the observed trends are qualitatively predicted within some theoretical models [41, 66–68].

Due to the different pseudorapidity coverage of LHCb with respect to other LHC experiments, the comparison of the measured BEC parameters for a given multiplicity out of a pp interaction is not straightforward. In the case of unfolded multiplicities in different pseudorapidity ranges quoted by experiments, the correspondence can be found using relations obtained from simulated events. The results for pp collisions at 7 TeV published by the ATLAS experiment [30] are quoted for unfolded multiplicities in the pseudorapidity range $|\eta| < 2.5$ and $p_T > 0.1$ GeV/ c . PYTHIA 8 is used to determine the relation for the multiplicity bins defined in the LHCb ($2 < \eta < 5$) and ATLAS ($|\eta| < 2.5$

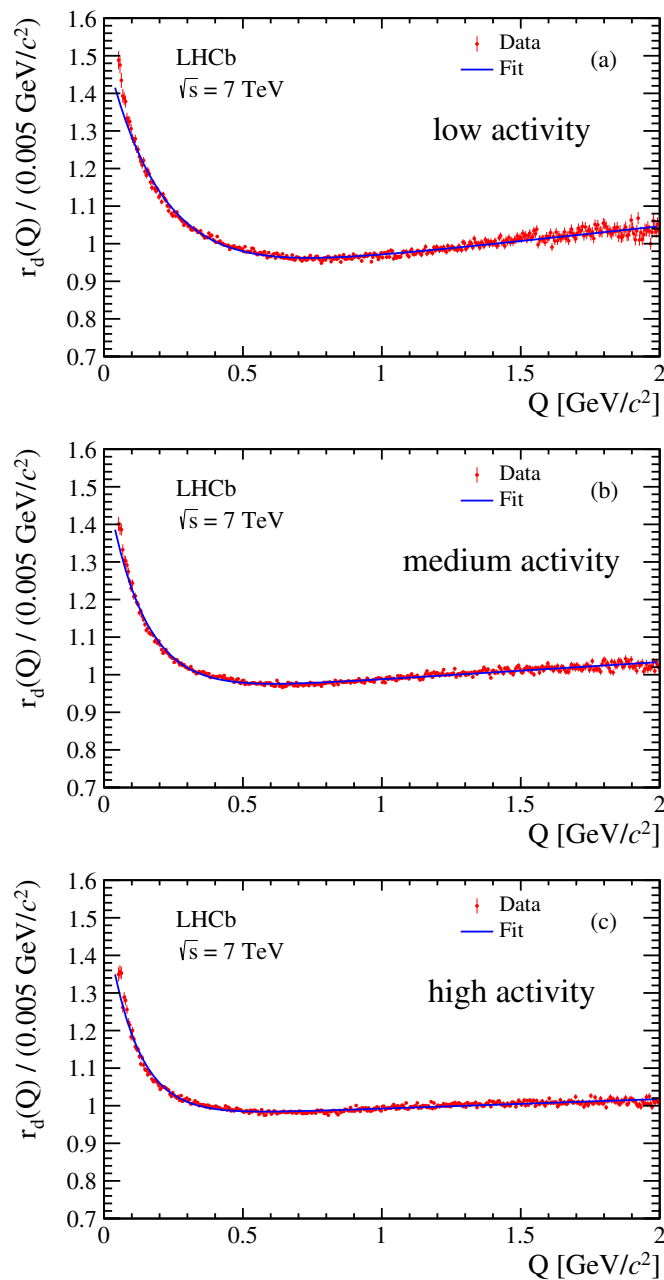


Figure 2. Results of the fit to the double ratio for like-sign pion pairs with event-mixed reference samples and the Coulomb effect subtracted for the three activity classes: (a) low, (b) medium and (c) high activity. The blue solid line denotes the fit result using the parameterisation of eq. (2.3). Only statistical uncertainties are shown.

and $p_T > 0.1 \text{ GeV}/c$ acceptances. The data indicate that the LHCb results for both R and λ are slightly below the ATLAS ones at 7 TeV. In order to perform a more detailed comparison it would be necessary to measure the BEC parameters using a full three-dimensional analysis [69].

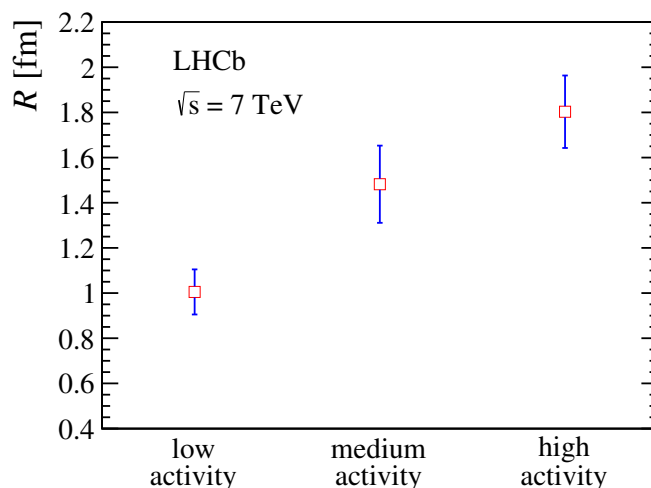


Figure 3. Correlation radius R as a function of activity. Error bars indicate the sum in quadrature of the statistical and systematic uncertainties. The points are placed at the centres of the activity bins.

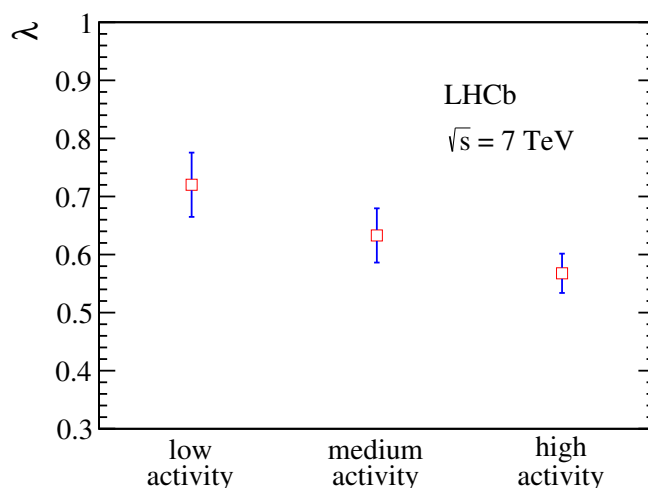


Figure 4. Chaoticity parameter λ as a function of activity. Error bars indicate the sum in quadrature of the statistical and systematic uncertainties. The points are placed at the centres of the activity bins.

It should be noted that the fit quality using the parameterisation, eq. (2.3), is poor (see figure 2). The χ^2 values are equal to 591, 623 and 621 for 386 degrees of freedom for low, medium and high activity classes, respectively. The difference between the fitted function and the data points, visible in the whole Q range, is particularly large in the low- Q BEC signal region below $0.2 \text{ GeV}/c^2$. This indicates that the approximate parameterisation of eq. (2.3) does not reproduce the measured distribution properly. Such an effect is observed also by other experiments [29, 30]. This may introduce an additional systematic uncertainty in the theoretical interpretation of the fit results.

7 Summary and conclusions

Using a data sample collected by the LHCb experiment in proton-proton collisions at a centre-of-mass energy of 7 TeV, the Bose-Einstein correlations between two indistinguishable pions are studied in the forward acceptance region of $2 < \eta < 5$ for single pions with transverse momentum $p_T > 0.1 \text{ GeV}/c$. An enhancement of pairs of same-sign charged pions with small relative momentum related to the BEC effect is observed. An event-mixed reference sample is used to determine the signal and the double ratio distributions are fitted using an exponential parameterisation. The results confirm that the effective size of the emission region increases as a function of increasing charged-particle multiplicity, while the chaoticity parameter decreases, as previously observed at LEP and at the other LHC experiments. The R and λ parameters measured in the forward region in three different charged-particle multiplicity bins are slightly lower with respect to those measured by ATLAS for corresponding pp interaction multiplicities.

Acknowledgments

We express our gratitude to our colleagues in the CERN accelerator departments for the excellent performance of the LHC. We thank the technical and administrative staff at the LHCb institutes. We acknowledge support from CERN and from the national agencies: CAPES, CNPq, FAPERJ and FINEP (Brazil); MOST and NSFC (China); CNRS/IN2P3 (France); BMBF, DFG and MPG (Germany); INFN (Italy); NWO (The Netherlands); MNiSW and NCN (Poland); MEN/IFA (Romania); MinES and FASO (Russia); MinECo (Spain); SNSF and SER (Switzerland); NASU (Ukraine); STFC (United Kingdom); NSF (USA). We acknowledge the computing resources that are provided by CERN, IN2P3 (France), KIT and DESY (Germany), INFN (Italy), SURF (The Netherlands), PIC (Spain), GridPP (United Kingdom), RRCKI and Yandex LLC (Russia), CSCS (Switzerland), IFIN-HH (Romania), CBPF (Brazil), PL-GRID (Poland) and OSC (USA). We are indebted to the communities behind the multiple open source software packages on which we depend. Individual groups or members have received support from AvH Foundation (Germany), EPLANET, Marie Skłodowska-Curie Actions and ERC (European Union), Conseil Général de Haute-Savoie, Labex ENIGMASS and OCEVU, Région Auvergne (France), RFBR and Yandex LLC (Russia), GVA, XuntaGal and GENCAT (Spain), Herchel Smith Fund, The Royal Society, Royal Commission for the Exhibition of 1851 and the Leverhulme Trust (United Kingdom).

Open Access. This article is distributed under the terms of the Creative Commons Attribution License ([CC-BY 4.0](https://creativecommons.org/licenses/by/4.0/)), which permits any use, distribution and reproduction in any medium, provided the original author(s) and source are credited.

References

- [1] T. Kanki, K. Kinoshita, H. Sumiyoshi and F. Takagi, *Multiparticle production in particle and nuclear collisions. I*, *Prog. Theor. Phys. Suppl.* **97A** (1988) 1 [*Erratum ibid.* **97B** (1989) 290].
- [2] D.H. Boal, C.K. Gelbke and B.K. Jennings, *Intensity interferometry in subatomic physics*, *Rev. Mod. Phys.* **62** (1990) 553 [INSPIRE].
- [3] R.H. Brown and R.Q. Twiss, *LXXIV. A new type of interferometer for use in radio astronomy*, *Phil. Mag.* **45** (1954) 663.
- [4] R.H. Brown and R.Q. Twiss, *Correlation between photons in two coherent beams of light*, *Nature* **177** (1956) 27 [INSPIRE].
- [5] R.H. Brown and R.Q. Twiss, *A test of a new type of stellar interferometer on Sirius*, *Nature* **178** (1956) 1046.
- [6] G. Goldhaber, W.B. Fowler, S. Goldhaber and T.F. Hoang, *Pion-pion correlations in antiproton annihilation events*, *Phys. Rev. Lett.* **3** (1959) 181 [INSPIRE].
- [7] ALEPH collaboration, D. Decamp et al., *A study of Bose-Einstein correlations in e^+e^- annihilation at 91 GeV*, *Z. Phys. C* **54** (1992) 75 [INSPIRE].
- [8] ALEPH collaboration, D. Buskulic et al., *Production of K^0 and Λ in hadronic Z decays*, *Z. Phys. C* **64** (1994) 361 [INSPIRE].
- [9] ALEPH collaboration, R. Barate et al., *Fermi-Dirac correlations in Λ pairs in hadronic Z decays*, *Phys. Lett. B* **475** (2000) 395 [INSPIRE].
- [10] ALEPH collaboration, A. Heister et al., *Two-dimensional analysis of Bose-Einstein correlations in hadronic Z decays at LEP*, *Eur. Phys. J. C* **36** (2004) 147 [INSPIRE].
- [11] DELPHI collaboration, P. Abreu et al., *Bose-Einstein correlations in the hadronic decays of the Z^0* , *Phys. Lett. B* **286** (1992) 201 [INSPIRE].
- [12] DELPHI collaboration, P. Abreu et al., *Kaon interference in the hadronic decays of the Z^0* , *Phys. Lett. B* **379** (1996) 330 [INSPIRE].
- [13] DELPHI collaboration, P. Abreu et al., *Two-dimensional analysis of the Bose-Einstein correlations in e^+e^- annihilation at the Z^0 peak*, *Phys. Lett. B* **471** (2000) 460 [INSPIRE].
- [14] L3 collaboration, M. Acciarri et al., *Measurement of an elongation of the pion source in Z decays*, *Phys. Lett. B* **458** (1999) 517 [hep-ex/9909009] [INSPIRE].
- [15] L3 collaboration, P. Achard et al., *Bose-Einstein correlations of neutral and charged pions in hadronic Z decays*, *Phys. Lett. B* **524** (2002) 55 [hep-ex/0109036] [INSPIRE].
- [16] L3 collaboration, P. Achard et al., *Test of the τ -model of Bose-Einstein correlations and reconstruction of the source function in hadronic Z-boson decay at LEP*, *Eur. Phys. J. C* **71** (2011) 1648 [arXiv:1105.4788] [INSPIRE].
- [17] OPAL collaboration, G. Abbiendi et al., *Bose-Einstein correlations in $K^\pm K^\pm$ pairs from Z^0 decays into two hadronic jets*, *Eur. Phys. J. C* **21** (2001) 23 [hep-ex/0001045] [INSPIRE].
- [18] OPAL collaboration, R. Akers et al., *The production of neutral kaons in Z^0 decays and their Bose-Einstein correlations*, *Z. Phys. C* **67** (1995) 389 [INSPIRE].
- [19] OPAL collaboration, G. Alexander et al., *Multiplicity dependence of Bose-Einstein correlations in hadronic Z^0 decays*, *Z. Phys. C* **72** (1996) 389 [INSPIRE].

- [20] OPAL collaboration, G. Abbiendi et al., *Transverse and longitudinal Bose-Einstein correlations in hadronic Z^0 decays*, *Eur. Phys. J. C* **16** (2000) 423 [[hep-ex/0002062](#)] [[INSPIRE](#)].
- [21] OPAL collaboration, G. Abbiendi et al., *Bose-Einstein correlations of π^0 pairs from hadronic Z^0 decays*, *Phys. Lett. B* **559** (2003) 131 [[hep-ex/0302027](#)] [[INSPIRE](#)].
- [22] H1 collaboration, C. Adloff et al., *Bose-Einstein correlations in deep inelastic ep scattering at HERA*, *Z. Phys. C* **75** (1997) 437 [[hep-ex/9705001](#)] [[INSPIRE](#)].
- [23] CERES collaboration, H. Tilsner and H. Appelshäuser, *Two-pion Bose-Einstein correlations at SPS energies*, *Nucl. Phys. A* **715** (2003) 607 [[INSPIRE](#)].
- [24] T. Alexopoulos et al., *A study of source size in $p\bar{p}$ collisions at $\sqrt{s} = 1.8$ TeV using pion interferometry*, *Phys. Rev. D* **48** (1993) 1931 [[INSPIRE](#)].
- [25] STAR collaboration, M.M. Aggarwal et al., *Pion femtoscopy in $p + p$ collisions at $\sqrt{s} = 200$ GeV*, *Phys. Rev. C* **83** (2011) 064905 [[arXiv:1004.0925](#)] [[INSPIRE](#)].
- [26] ALICE collaboration, *Femtoscopy of pp collisions at $\sqrt{s} = 0.9$ and 7 TeV at the LHC with two-pion Bose-Einstein correlations*, *Phys. Rev. D* **84** (2011) 112004 [[arXiv:1101.3665](#)] [[INSPIRE](#)].
- [27] ALICE collaboration, *$K_s^0 - K_s^0$ correlations in pp collisions at $\sqrt{s} = 7$ TeV from the LHC ALICE experiment*, *Phys. Lett. B* **717** (2012) 151 [[arXiv:1206.2056](#)] [[INSPIRE](#)].
- [28] CMS collaboration, *First measurement of Bose-Einstein correlations in proton-proton collisions at $\sqrt{s} = 0.9$ and 2.36 TeV at the LHC*, *Phys. Rev. Lett.* **105** (2010) 032001 [[arXiv:1005.3294](#)] [[INSPIRE](#)].
- [29] CMS collaboration, *Measurement of Bose-Einstein correlations in pp collisions at $\sqrt{s} = 0.9$ and 7 TeV*, *JHEP* **05** (2011) 029 [[arXiv:1101.3518](#)] [[INSPIRE](#)].
- [30] ATLAS collaboration, *Two-particle Bose-Einstein correlations in pp collisions at $\sqrt{s} = 0.9$ and 7 TeV measured with the ATLAS detector*, *Eur. Phys. J. C* **75** (2015) 466 [[arXiv:1502.07947](#)] [[INSPIRE](#)].
- [31] CMS collaboration, *Bose-Einstein correlation measurements at CMS*, *Nucl. Phys. A* **931** (2014) 1061 [[INSPIRE](#)].
- [32] ALICE collaboration, *Two-pion Bose-Einstein correlations in central Pb-Pb collisions at $\sqrt{s_{NN}} = 2.76$ TeV*, *Phys. Lett. B* **696** (2011) 328 [[arXiv:1012.4035](#)] [[INSPIRE](#)].
- [33] G. Alexander, I. Cohen and E. Levin, *The dependence of the emission size on the hadron mass*, *Phys. Lett. B* **452** (1999) 159 [[hep-ph/9901341](#)] [[INSPIRE](#)].
- [34] A. Bialas and K. Zalewski, *Mass dependence of the HBT radii observed in e^+e^- annihilation*, *Acta Phys. Polon.* **30** (1999) 359 [[hep-ph/9901382](#)] [[INSPIRE](#)].
- [35] A. Bialas, M. Kucharczyk, H. Palka and K. Zalewski, *Mass dependence of HBT correlations in e^+e^- annihilation*, *Phys. Rev. D* **62** (2000) 114007 [[hep-ph/0006290](#)] [[INSPIRE](#)].
- [36] A. Bialas, M. Kucharczyk, H. Palka and K. Zalewski, *Mass dependence of HBT correlations in e^+e^- annihilation. II*, *Acta Phys. Polon.* **32** (2001) 2901 [[INSPIRE](#)].
- [37] G. Baym, *The physics of Hanbury Brown-Twiss intensity interferometry: from stars to nuclear collisions*, *Acta Phys. Polon.* **29** (1998) 1839 [[nucl-th/9804026](#)] [[INSPIRE](#)].
- [38] B. Lorstad, *Boson interferometry — a review of high-energy data and its interpretation*, *Int. J. Mod. Phys. A* **4** (1989) 2861 [[INSPIRE](#)].

- [39] T. Csorgo, S. Hegyi and W.A. Zajc, *Bose-Einstein correlations for Levy stable source distributions*, *Eur. Phys. J. C* **36** (2004) 67 [[nuc1-th/0310042](#)] [[INSPIRE](#)].
- [40] M. Deutschmann et al., *A study of second order interference for pions produced in various hadronic interactions*, *Nucl. Phys. B* **204** (1982) 333 [[INSPIRE](#)].
- [41] W. Kittel and E.A. DeWolf, *Soft multihadron dynamics*, World Scientific, Singapore (2005) [[ISBN:978-981-256-295-1](#)].
- [42] G.I. Kopylov, *Like particle correlations as a tool to study the multiple production mechanism*, *Phys. Lett.* **50B** (1974) 472 [[INSPIRE](#)].
- [43] B. Andersson, G. Gustafson, G. Ingelman and T. Sjöstrand, *Parton fragmentation and string dynamics*, *Phys. Rept.* **97** (1983) 31 [[INSPIRE](#)].
- [44] M. Gyulassy, S.K. Kauffmann and L.W. Wilson, *Pion interferometry of nuclear collisions. 1. Theory*, *Phys. Rev. C* **20** (1979) 2267 [[INSPIRE](#)].
- [45] S. Pratt, *Coherence and coulomb effects on pion interferometry*, *Phys. Rev. D* **33** (1986) 72 [[INSPIRE](#)].
- [46] LHCb collaboration, *The LHCb detector at the LHC*, 2008 *JINST* **3** S08005 [[INSPIRE](#)].
- [47] R. Aaij et al., *Performance of the LHCb Vertex Locator*, 2014 *JINST* **9** 09007 [[arXiv:1405.7808](#)] [[INSPIRE](#)].
- [48] LHCb OUTER TRACKER GROUP collaboration, *Performance of the LHCb Outer Tracker*, 2014 *JINST* **9** P01002 [[arXiv:1311.3893](#)] [[INSPIRE](#)].
- [49] LHCb RICH GROUP collaboration, *Performance of the LHCb RICH detector at the LHC*, *Eur. Phys. J. C* **73** (2013) 2431 [[arXiv:1211.6759](#)] [[INSPIRE](#)].
- [50] A.A. Alves, Jr. et al., *Performance of the LHCb muon system*, 2013 *JINST* **8** P02022 [[arXiv:1211.1346](#)] [[INSPIRE](#)].
- [51] R. Aaij et al., *The LHCb trigger and its performance in 2011*, 2013 *JINST* **8** P04022 [[arXiv:1211.3055](#)] [[INSPIRE](#)].
- [52] LHCb collaboration, *Precision luminosity measurements at LHCb*, 2014 *JINST* **9** P12005 [[arXiv:1410.0149](#)] [[INSPIRE](#)].
- [53] T. Sjöstrand, S. Mrenna and P.Z. Skands, *A brief introduction to PYTHIA 8.1*, *Comput. Phys. Commun.* **178** (2008) 852 [[arXiv:0710.3820](#)] [[INSPIRE](#)].
- [54] LHCb collaboration, *Handling of the generation of primary events in Gauss, the LHCb simulation framework*, *J. Phys. Conf. Ser.* **331** (2011) 032047 [[INSPIRE](#)].
- [55] D.J. Lange, *The EvtGen particle decay simulation package*, *Nucl. Instrum. Meth. A* **462** (2001) 152 [[INSPIRE](#)].
- [56] P. Golonka and Z. Was, *PHOTOS Monte Carlo: a precision tool for QED corrections in Z and W decays*, *Eur. Phys. J. C* **45** (2006) 97 [[hep-ph/0506026](#)] [[INSPIRE](#)].
- [57] GEANT4 collaboration, J. Allison et al., *Geant4 developments and applications*, *IEEE Trans. Nucl. Sci.* **53** (2006) 270.
- [58] GEANT4 collaboration, S. Agostinelli et al., *GEANT4: a simulation toolkit*, *Nucl. Instrum. Meth. A* **506** (2003) 250 [[INSPIRE](#)].
- [59] LHCb collaboration, *The LHCb simulation application, Gauss: Design, evolution and experience*, *J. Phys. Conf. Ser.* **331** (2011) 032023 [[INSPIRE](#)].

- [60] T. Sjöstrand, S. Mrenna and P.Z. Skands, *PYTHIA 6.4 physics and manual*, *JHEP* **05** (2006) 026 [[hep-ph/0603175](#)] [[INSPIRE](#)].
- [61] P.Z. Skands, *The Perugia tunes*, [arXiv:0905.3418](#) [[INSPIRE](#)].
- [62] A. Powell et al., *Particle identification at LHCb*, [LHCb-PROC-2011-008](#) (2011).
- [63] G. D'Agostini, *A multidimensional unfolding method based on Bayes' theorem*, *Nucl. Instrum. Meth. A* **362** (1995) 487 [[INSPIRE](#)].
- [64] LHCb collaboration, *Measurement of charged particle multiplicities and densities in pp collisions at $\sqrt{s} = 7$ TeV in the forward region*, *Eur. Phys. J. C* **74** (2014) 2888 [[arXiv:1402.4430](#)] [[INSPIRE](#)].
- [65] S. Kullback and R. Leibler, *On information and sufficiency*, *Ann. Math. Statist.* **22** (1951) 79.
- [66] N. Suzuki and M. Biyajima, *Multiplicity dependence of identical particle correlations in the quantum optical approach*, *Phys. Rev. C* **60** (1999) 034903 [[hep-ph/9907348](#)] [[INSPIRE](#)].
- [67] B. Buschbeck, H.C. Eggers and P. Lipa, *Multiplicity dependence of correlation functions in $\bar{p}p$ reactions at $\sqrt{s} = 630$ GeV*, *Phys. Lett. B* **481** (2000) 187 [[hep-ex/0003029](#)] [[INSPIRE](#)].
- [68] G. Alexander and E. Sarkisian, *The effect of many sources on the genuine multiparticle correlations*, *Phys. Lett. B* **487** (2000) 215 [[hep-ph/0005212](#)] [[INSPIRE](#)].
- [69] K. Geiger, J. Ellis, U. Heinz, and U.A. Wiedemann, *Bose-Einstein correlations in a space-time approach to e^+e^- annihilation into hadrons*, *Phys. Rev. D* **61** (2000) 054002 [[hep-ph/9811270](#)] [[INSPIRE](#)].

The LHCb collaboration

R. Aaij⁴⁰, B. Adeva³⁹, M. Adinolfi⁴⁸, Z. Ajaltouni⁵, S. Akar⁵⁹, J. Albrecht¹⁰, F. Alessio⁴⁰, M. Alexander⁵³, A. Alfonso Alberio³⁸, S. Ali⁴³, G. Alkhazov³¹, P. Alvarez Cartelle⁵⁵, A.A. Alves Jr⁵⁹, S. Amato², S. Amerio²³, Y. Amhis⁷, L. An³, L. Anderlini¹⁸, G. Andreassi⁴¹, M. Andreotti^{17,g}, J.E. Andrews⁶⁰, R.B. Appleby⁵⁶, F. Archilli⁴³, P. d'Argent¹², J. Arnau Romeu⁶, A. Artamonov³⁷, M. Artuso⁶¹, E. Aslanides⁶, G. Auremma²⁶, M. Baalouch⁵, I. Babuschkin⁵⁶, S. Bachmann¹², J.J. Back⁵⁰, A. Badalov^{38,m}, C. Baesso⁶², S. Baker⁵⁵, V. Balagura^{7,b}, W. Baldini¹⁷, A. Baranov³⁵, R.J. Barlow⁵⁶, C. Barschel⁴⁰, S. Barsuk⁷, W. Barter⁵⁶, F. Baryshnikov³², V. Batozskaya²⁹, V. Battista⁴¹, A. Bay⁴¹, L. Beaucourt⁴, J. Beddow⁵³, F. Bedeschi²⁴, I. Bediaga¹, A. Beiter⁶¹, L.J. Bel⁴³, N. Belyi⁶³, V. Bellee⁴¹, N. Belloli^{21,i}, K. Belous³⁷, I. Belyaev³², E. Ben-Haim⁸, G. Bencivenni¹⁹, S. Benson⁴³, S. Beranek⁹, A. Berezhnoy³³, R. Bernet⁴², D. Berninghoff¹², E. Bertholet⁸, A. Bertolin²³, C. Betancourt⁴², F. Betti¹⁵, M.-O. Bettler⁴⁰, M. van Beuzekom⁴³, I.A. Bezshyiko⁴², S. Bifani⁴⁷, P. Billoir⁸, A. Birnkraut¹⁰, A. Bitadze⁵⁶, A. Bizzeti^{18,u}, M. Björn⁵⁷, T. Blake⁵⁰, F. Blanc⁴¹, J. Blouw^{11,†}, S. Blusk⁶¹, V. Bocci²⁶, T. Boettcher⁵⁸, A. Bondar^{36,w}, N. Bondar³¹, W. Bonivento¹⁶, I. Bordyuzhin³², A. Borgheresi^{21,i}, S. Borghi⁵⁶, M. Borisyak³⁵, M. Borsato³⁹, F. Bossu⁷, M. Boubdir⁹, T.J.V. Bowcock⁵⁴, E. Bowen⁴², C. Bozzi^{17,40}, S. Braun¹², T. Britton⁶¹, J. Brodzicka²⁷, D. Brundu¹⁶, E. Buchanan⁴⁸, C. Burr⁵⁶, A. Bursche^{16,f}, J. Buytaert⁴⁰, W. Byczynski⁴⁰, S. Cadeddu¹⁶, H. Cai⁶⁴, R. Calabrese^{17,g}, R. Calladine⁴⁷, M. Calvi^{21,i}, M. Calvo Gomez^{38,m}, A. Camboni^{38,m}, P. Campana¹⁹, D.H. Campora Perez⁴⁰, L. Capriotti⁵⁶, A. Carbone^{15,e}, G. Carboni^{25,j}, R. Cardinale^{20,h}, A. Cardini¹⁶, P. Carniti^{21,i}, L. Carson⁵², K. Carvalho Akiba², G. Casse⁵⁴, L. Cassina²¹, L. Castillo Garcia⁴¹, M. Cattaneo⁴⁰, G. Cavallero^{20,40,h}, R. Cenci^{24,t}, D. Chamont⁷, M. Charles⁸, Ph. Charpentier⁴⁰, G. Chatzikonstantinidis⁴⁷, M. Chefdeville⁴, S. Chen⁵⁶, S.F. Cheung⁵⁷, S.-G. Chitic⁴⁰, V. Chobanova³⁹, M. Chrzaszcz^{42,27}, A. Chubykin³¹, P. Ciambone¹⁹, X. Cid Vidal³⁹, G. Ciezarek⁴³, P.E.L. Clarke⁵², M. Clemencic⁴⁰, H.V. Cliff⁴⁹, J. Closier⁴⁰, J. Cogan⁶, E. Cogneras⁵, V. Cogoni^{16,f}, L. Cojocariu³⁰, P. Collins⁴⁰, T. Colombo⁴⁰, A. Comerma-Montells¹², A. Contu⁴⁰, A. Cook⁴⁸, G. Coombs⁴⁰, S. Coquereau³⁸, G. Corti⁴⁰, M. Corvo^{17,g}, C.M. Costa Sobral⁵⁰, B. Couturier⁴⁰, G.A. Cowan⁵², D.C. Craik⁵⁸, A. Crocombe⁵⁰, M. Cruz Torres¹, R. Currie⁵², C. D'Ambrosio⁴⁰, F. Da Cunha Marinho², E. Dall'Occo⁴³, J. Dalseno⁴⁸, A. Davis³, O. De Aguiar Francisco⁵⁴, S. De Capua⁵⁶, M. De Cian¹², J.M. De Miranda¹, L. De Paula², M. De Serio^{14,d}, P. De Simone¹⁹, C.T. Dean⁵³, D. Decamp⁴, L. Del Buono⁸, H.-P. Dembinski¹¹, M. Demmer¹⁰, A. Dendek²⁸, D. Derkach³⁵, O. Deschamps⁵, F. Dettori⁵⁴, B. Dey⁶⁵, A. Di Canto⁴⁰, P. Di Nezza¹⁹, H. Dijkstra⁴⁰, F. Dordei⁴⁰, M. Dorigo⁴⁰, A. Dosil Suárez³⁹, L. Douglas⁵³, A. Dovbnya⁴⁵, K. Dreimanis⁵⁴, L. Dufour⁴³, G. Dujany⁸, P. Durante⁴⁰, R. Dzhelyadin³⁷, M. Dziewiecki¹², A. Dziurda⁴⁰, A. Dzyuba³¹, S. Easo⁵¹, M. Ebert⁵², U. Egede⁵⁵, V. Egorychev³², S. Eidelman^{36,w}, S. Eisenhardt⁵², U. Eitschberger¹⁰, R. Ekelhof¹⁰, L. Eklund⁵³, S. Ely⁶¹, S. Esen¹², H.M. Evans⁴⁹, T. Evans⁵⁷, A. Falabella¹⁵, N. Farley⁴⁷, S. Farry⁵⁴, D. Fazzini^{21,i}, L. Federici²⁵, D. Ferguson⁵², G. Fernandez³⁸, P. Fernandez Declara⁴⁰, A. Fernandez Prieto³⁹, F. Ferrari¹⁵, F. Ferreira Rodrigues², M. Ferro-Luzzi⁴⁰, S. Filippov³⁴, R.A. Fini¹⁴, M. Fiore^{17,g}, M. Fiorini^{17,g}, M. Firlej²⁸, C. Fitzpatrick⁴¹, T. Fiutowski²⁸, F. Fleuret^{7,b}, K. Fohl⁴⁰, M. Fontana^{16,40}, F. Fontanelli^{20,h}, D.C. Forshaw⁶¹, R. Forty⁴⁰, V. Franco Lima⁵⁴, M. Frank⁴⁰, C. Frei⁴⁰, J. Fu^{22,q}, W. Funk⁴⁰, E. Furfaro^{25,j}, C. Färber⁴⁰, E. Gabriel⁵², A. Gallas Torreira³⁹, D. Galli^{15,e}, S. Gallorini²³, S. Gambetta⁵², M. Gandelman², P. Gandini⁵⁷, Y. Gao³, L.M. Garcia Martin⁷⁰, J. García Pardiñas³⁹, J. Garra Tico⁴⁹, L. Garrido³⁸, P.J. Garsed⁴⁹, D. Gascon³⁸, C. Gaspar⁴⁰, L. Gavardi¹⁰, G. Gazzoni⁵, D. Gerick¹², E. Gersabeck¹², M. Gersabeck⁵⁶, T. Gershon⁵⁰,

Ph. Ghez⁴, S. Giani⁴¹, V. Gibson⁴⁹, O.G. Girard⁴¹, L. Giubega³⁰, K. Gizdov⁵², V.V. Gligorov⁸, D. Golubkov³², A. Golutvin^{55,40}, A. Gomes^{1,a}, I.V. Gorelov³³, C. Gotti^{21,i}, E. Govorkova⁴³, J.P. Grabowski¹², R. Graciani Diaz³⁸, L.A. Granado Cardoso⁴⁰, E. Graugés³⁸, E. Graverini⁴², G. Graziani¹⁸, A. Grecu³⁰, R. Greim⁹, P. Griffith¹⁶, L. Grillo^{21,40,i}, L. Gruber⁴⁰, B.R. Gruberg Cazon⁵⁷, O. Grünberg⁶⁷, E. Gushchin³⁴, Yu. Guz³⁷, T. Gys⁴⁰, C. Göbel⁶², T. Hadavizadeh⁵⁷, C. Hadjivasiliou⁵, G. Haefeli⁴¹, C. Haen⁴⁰, S.C. Haines⁴⁹, B. Hamilton⁶⁰, X. Han¹², T.H. Hancock⁵⁷, S. Hansmann-Menzemer¹², N. Harnew⁵⁷, S.T. Harnew⁴⁸, J. Harrison⁵⁶, C. Hasse⁴⁰, M. Hatch⁴⁰, J. He⁶³, M. Hecker⁵⁵, K. Heinicke¹⁰, A. Heister⁹, K. Hennessy⁵⁴, P. Henrard⁵, L. Henry⁷⁰, E. van Herwijnen⁴⁰, M. Heß⁶⁷, A. Hicheur², D. Hill⁵⁷, C. Hombach⁵⁶, P.H. Hopchev⁴¹, Z.C. Huard⁵⁹, W. Hulsbergen⁴³, T. Humair⁵⁵, M. Hushchyn³⁵, D. Hutchcroft⁵⁴, P. Ibis¹⁰, M. Idzik²⁸, P. Ilten⁵⁸, R. Jacobsson⁴⁰, J. Jalocha⁵⁷, E. Jans⁴³, A. Jawahery⁶⁰, M. Jezabek²⁷, F. Jiang³, M. John⁵⁷, D. Johnson⁴⁰, C.R. Jones⁴⁹, C. Joram⁴⁰, B. Jost⁴⁰, N. Jurik⁵⁷, S. Kandybei⁴⁵, M. Karacson⁴⁰, J.M. Kariuki⁴⁸, S. Karodia⁵³, N. Kazeev³⁵, M. Kecke¹², M. Kelsey⁶¹, M. Kenzie⁴⁹, T. Ketel⁴⁴, E. Khairullin³⁵, B. Khanji¹², C. Khurewathanakul⁴¹, T. Kirn⁹, S. Klaver⁵⁶, K. Klimaszewski²⁹, T. Klimkovich¹¹, S. Koliiev⁴⁶, M. Kolpin¹², I. Komarov⁴¹, R. Kopecka¹², P. Koppenburg⁴³, A. Kosmyntseva³², S. Kotriakhova³¹, M. Kozeiha⁵, L. Kravchuk³⁴, M. Kreps⁵⁰, P. Krokovny^{36,w}, F. Kruse¹⁰, W. Krzemien²⁹, W. Kucewicz^{27,l}, M. Kucharczyk²⁷, V. Kudryavtsev^{36,w}, A.K. Kuonen⁴¹, K. Kurek²⁹, T. Kvaratskheliya^{32,40}, D. Lacarrere⁴⁰, G. Lafferty⁵⁶, A. Lai¹⁶, G. Lanfranchi¹⁹, C. Langenbruch⁹, T. Latham⁵⁰, C. Lazzeroni⁴⁷, R. Le Gac⁶, A. Leflat^{33,40}, J. Lefrançois⁷, R. Lefèvre⁵, F. Lemaitre⁴⁰, E. Lemos Cid³⁹, O. Leroy⁶, T. Lesiak²⁷, B. Leverington¹², P.-R. Li⁶³, T. Li³, Y. Li⁷, Z. Li⁶¹, T. Likhomanenko⁶⁸, R. Lindner⁴⁰, F. Lionetto⁴², V. Lisovskyi⁷, X. Liu³, D. Loh⁵⁰, A. Loi¹⁶, I. Longstaff⁵³, J.H. Lopes², D. Lucchesi^{23,o}, M. Lucio Martinez³⁹, H. Luo⁵², A. Lupato²³, E. Luppi^{17,g}, O. Lupton⁴⁰, A. Lusiani²⁴, X. Lyu⁶³, F. Machefert⁷, F. Maciuc³⁰, V. Macko⁴¹, P. Mackowiak¹⁰, S. Maddrell-Mander⁴⁸, O. Maev^{31,40}, K. Maguire⁵⁶, D. Maisuzenko³¹, M.W. Majewski²⁸, S. Malde⁵⁷, B. Malecki²⁷, A. Malinin⁶⁸, T. Maltsev^{36,w}, G. Manca^{16,f}, G. Mancinelli⁶, P. Manning⁶¹, D. Marangotto^{22,q}, J. Maratas^{5,v}, J.F. Marchand⁴, U. Marconi¹⁵, C. Marin Benito³⁸, M. Marinangeli⁴¹, P. Marino⁴¹, J. Marks¹², G. Martellotti²⁶, M. Martin⁶, M. Martinelli⁴¹, D. Martinez Santos³⁹, F. Martinez Vidal⁷⁰, D. Martins Tostes², L.M. Massacrier⁷, A. Massafferri¹, R. Matev⁴⁰, A. Mathad⁵⁰, Z. Mathe⁴⁰, C. Matteuzzi²¹, A. Mauri⁴², E. Maurice^{7,b}, B. Maurin⁴¹, A. Mazurov⁴⁷, M. McCann^{55,40}, A. McNab⁵⁶, R. McNulty¹³, J.V. Mead⁵⁴, B. Meadows⁵⁹, C. Meaux⁶, F. Meier¹⁰, N. Meinert⁶⁷, D. Melnychuk²⁹, M. Merk⁴³, A. Merli^{22,40,q}, E. Michielin²³, D.A. Milanes⁶⁶, E. Millard⁵⁰, M.-N. Minard⁴, L. Minzoni¹⁷, D.S. Mitzel¹², A. Mogini⁸, J. Molina Rodriguez¹, T. Mombächer¹⁰, I.A. Monroy⁶⁶, S. Monteil⁵, M. Morandin²³, M.J. Morello^{24,t}, O. Morgunova⁶⁸, J. Moron²⁸, A.B. Morris⁵², R. Mountain⁶¹, F. Muheim⁵², M. Mulder⁴³, D. Müller⁵⁶, J. Müller¹⁰, K. Müller⁴², V. Müller¹⁰, P. Naik⁴⁸, T. Nakada⁴¹, R. Nandakumar⁵¹, A. Nandi⁵⁷, I. Nasteva², M. Needham⁵², N. Neri^{22,40}, S. Neubert¹², N. Neufeld⁴⁰, M. Neuner¹², T.D. Nguyen⁴¹, C. Nguyen-Mau^{41,n}, S. Nieswand⁹, R. Niet¹⁰, N. Nikitin³³, T. Nikodem¹², A. Nogay⁶⁸, D.P. O’Hanlon⁵⁰, A. Oblakowska-Mucha²⁸, V. Obraztsov³⁷, S. Ogilvy¹⁹, R. Oldeman^{16,f}, C.J.G. Onderwater⁷¹, A. Ossowska²⁷, J.M. Otalora Goicochea², P. Owen⁴², A. Oyanguren⁷⁰, P.R. Pais⁴¹, A. Palano^{14,d}, M. Palutan^{19,40}, A. Papanestis⁵¹, M. Pappagallo^{14,d}, L.L. Pappalardo^{17,g}, W. Parker⁶⁰, C. Parkes⁵⁶, G. Passaleva¹⁸, A. Pastore^{14,d}, M. Patel⁵⁵, C. Patrignani^{15,e}, A. Pearce⁴⁰, A. Pellegrino⁴³, G. Penso²⁶, M. Pepe Altarelli⁴⁰, S. Perazzini⁴⁰, P. Perret⁵, L. Pescatore⁴¹, K. Petridis⁴⁸, A. Petrolini^{20,h}, A. Petrov⁶⁸, M. Petruzzio^{22,q}, E. Picatoste Olloqui³⁸, B. Pietrzyk⁴, M. Pikies²⁷, D. Pinci²⁶, F. Pisani⁴⁰, A. Pistone^{20,h}, A. Piucci¹², V. Placinta³⁰, S. Playfer⁵², M. Plo Casasus³⁹, F. Polci⁸, M. Poli Lener¹⁹, A. Poluektov^{50,36}, I. Polyakov⁶¹, E. Polcarpo², G.J. Pomery⁴⁸, S. Ponce⁴⁰, A. Popov³⁷, D. Popov^{11,40}, S. Poslavskii³⁷, C. Potterat², E. Price⁴⁸,

J. Prisciandaro³⁹, C. Prouve⁴⁸, V. Pugatch⁴⁶, A. Puig Navarro⁴², H. Pullen⁵⁷, G. Punzi^{24,p}, W. Qian⁵⁰, R. Quagliani^{7,48}, B. Quintana⁵, B. Rachwal²⁸, J.H. Rademacker⁴⁸, M. Rama²⁴, M. Ramos Pernas³⁹, M.S. Rangel², I. Raniuk^{45,†}, F. Ratnikov³⁵, G. Raven⁴⁴, M. Ravonel Salzgeber⁴⁰, M. Reboud⁴, F. Redi⁵⁵, S. Reichert¹⁰, A.C. dos Reis¹, C. Remon Alepuz⁷⁰, V. Renaudin⁷, S. Ricciardi⁵¹, S. Richards⁴⁸, M. Rihl⁴⁰, K. Rinnert⁵⁴, V. Rives Molina³⁸, P. Robbe⁷, A. Robert⁸, A.B. Rodrigues¹, E. Rodrigues⁵⁹, J.A. Rodriguez Lopez⁶⁶, P. Rodriguez Perez^{56,†}, A. Rogozhnikov³⁵, S. Roiser⁴⁰, A. Rollings⁵⁷, V. Romanovskiy³⁷, A. Romero Vidal³⁹, J.W. Ronayne¹³, M. Rotondo¹⁹, M.S. Rudolph⁶¹, T. Ruf⁴⁰, P. Ruiz Valls⁷⁰, J. Ruiz Vidal⁷⁰, J.J. Saborido Silva³⁹, E. Sadykhov³², N. Sagidova³¹, B. Saitta^{16,f}, V. Salustino Guimaraes¹, C. Sanchez Mayordomo⁷⁰, B. Sanmartin Sedes³⁹, R. Santacesaria²⁶, C. Santamarina Rios³⁹, M. Santimaria¹⁹, E. Santovetti^{25,j}, G. Sarpis⁵⁶, A. Sarti²⁶, C. Satriano^{26,s}, A. Satta²⁵, D.M. Saunders⁴⁸, D. Savrina^{32,33}, S. Schael⁹, M. Schellenberg¹⁰, M. Schiller⁵³, H. Schindler⁴⁰, M. Schlupp¹⁰, M. Schmelling¹¹, T. Schmelzer¹⁰, B. Schmidt⁴⁰, O. Schneider⁴¹, A. Schopper⁴⁰, H.F. Schreiner⁵⁹, K. Schubert¹⁰, M. Schubiger⁴¹, M.-H. Schune⁷, R. Schwemmer⁴⁰, B. Sciascia¹⁹, A. Sciubba^{26,k}, A. Semennikov³², E.S. Sepulveda⁸, A. Sergi⁴⁷, N. Serra⁴², J. Serrano⁶, L. Sestini²³, P. Seyfert⁴⁰, M. Shapkin³⁷, I. Shapoval⁴⁵, Y. Shcheglov³¹, T. Shears⁵⁴, L. Shekhtman^{36,w}, V. Shevchenko⁶⁸, B.G. Siddi^{17,40}, R. Silva Coutinho⁴², L. Silva de Oliveira², G. Simi^{23,o}, S. Simone^{14,d}, M. Sirendi⁴⁹, N. Skidmore⁴⁸, T. Skwarnicki⁶¹, E. Smith⁵⁵, I.T. Smith⁵², J. Smith⁴⁹, M. Smith⁵⁵, I. Soares Lavra¹, M.D. Sokoloff⁵⁹, F.J.P. Soler⁵³, B. Souza De Paula², B. Spaan¹⁰, P. Spradlin⁵³, S. Sridharan⁴⁰, F. Stagni⁴⁰, M. Stahl¹², S. Stahl⁴⁰, P. Stefko⁴¹, S. Stefkova⁵⁵, O. Steinkamp⁴², S. Stemmler¹², O. Stenyakin³⁷, M. Stepanova³¹, H. Stevens¹⁰, S. Stone⁶¹, B. Storaci⁴², S. Stracka^{24,p}, M.E. Stramaglia⁴¹, M. Straticiu³⁰, U. Straumann⁴², J. Sun³, L. Sun⁶⁴, W. Sutcliffe⁵⁵, K. Swientek²⁸, V. Syropoulos⁴⁴, M. Szczekowski²⁹, T. Szumlak²⁸, M. Szymanski⁶³, S. T'Jampens⁴, A. Tayduganov⁶, T. Tekampe¹⁰, G. Tellarini^{17,g}, F. Teubert⁴⁰, E. Thomas⁴⁰, J. van Tilburg⁴³, M.J. Tilley⁵⁵, V. Tisserand⁴, M. Tobin⁴¹, S. Tolk⁴⁹, L. Tomassetti^{17,g}, D. Tonelli²⁴, F. Toriello⁶¹, R. Tourinho Jadallah Aoude¹, E. Tournefier⁴, M. Traill⁵³, M.T. Tran⁴¹, M. Tresch⁴², A. Trisovic⁴⁰, A. Tsaregorodtsev⁶, P. Tsopelas⁴³, A. Tully⁴⁹, N. Tuning^{43,40}, A. Ukleja²⁹, A. Usachov⁷, A. Ustyuzhanin³⁵, U. Uwer¹², C. Vacca^{16,f}, A. Vagner⁶⁹, V. Vagnoni^{15,40}, A. Valassi⁴⁰, S. Valat⁴⁰, G. Valenti¹⁵, R. Vazquez Gomez¹⁹, P. Vazquez Regueiro³⁹, S. Vecchi¹⁷, M. van Veghel⁴³, J.J. Velthuis⁴⁸, M. Veltri^{18,r}, G. Veneziano⁵⁷, A. Venkateswaran⁶¹, T.A. Verlage⁹, M. Vernet⁵, M. Vesterinen⁵⁷, J.V. Viana Barbosa⁴⁰, B. Viaud⁷, D. Vieira⁶³, M. Vieites Diaz³⁹, H. Viemann⁶⁷, X. Vilasis-Cardona^{38,m}, M. Vitti⁴⁹, V. Volkov³³, A. Vollhardt⁴², B. Voneki⁴⁰, A. Vorobyev³¹, V. Vorobyev^{36,w}, C. Voß⁹, J.A. de Vries⁴³, C. Vázquez Sierra³⁹, R. Waldi⁶⁷, C. Wallace⁵⁰, R. Wallace¹³, J. Walsh²⁴, J. Wang⁶¹, D.R. Ward⁴⁹, H.M. Wark⁵⁴, N.K. Watson⁴⁷, D. Websdale⁵⁵, A. Weiden⁴², M. Whitehead⁴⁰, J. Wicht⁵⁰, G. Wilkinson^{57,40}, M. Wilkinson⁶¹, M. Williams⁵⁶, M.P. Williams⁴⁷, M. Williams⁵⁸, T. Williams⁴⁷, F.F. Wilson⁵¹, J. Wimberley⁶⁰, M. Winn⁷, J. Wishahi¹⁰, W. Wislicki²⁹, M. Witek²⁷, G. Wormser⁷, S.A. Wotton⁴⁹, K. Wraight⁵³, K. Wyllie⁴⁰, Y. Xie⁶⁵, Z. Xu⁴, Z. Yang³, Z. Yang⁶⁰, Y. Yao⁶¹, H. Yin⁶⁵, J. Yu⁶⁵, X. Yuan⁶¹, O. Yushchenko³⁷, K.A. Zarebski⁴⁷, M. Zavertyaev^{11,c}, L. Zhang³, Y. Zhang⁷, A. Zhelezov¹², Y. Zheng⁶³, X. Zhu³, V. Zhukov³³, J.B. Zonneveld⁵², S. Zucchelli¹⁵.

¹ Centro Brasileiro de Pesquisas Físicas (CBPF), Rio de Janeiro, Brazil

² Universidade Federal do Rio de Janeiro (UFRJ), Rio de Janeiro, Brazil

³ Center for High Energy Physics, Tsinghua University, Beijing, China

⁴ LAPP, Université Savoie Mont-Blanc, CNRS/IN2P3, Annecy-Le-Vieux, France

⁵ Clermont Université, Université Blaise Pascal, CNRS/IN2P3, LPC, Clermont-Ferrand, France

⁶ Aix Marseille Univ, CNRS/IN2P3, CPPM, Marseille, France

⁷ LAL, Université Paris-Sud, CNRS/IN2P3, Orsay, France

- ⁸ LPNHE, Université Pierre et Marie Curie, Université Paris Diderot, CNRS/IN2P3, Paris, France
- ⁹ I. Physikalisches Institut, RWTH Aachen University, Aachen, Germany
- ¹⁰ Fakultät Physik, Technische Universität Dortmund, Dortmund, Germany
- ¹¹ Max-Planck-Institut für Kernphysik (MPIK), Heidelberg, Germany
- ¹² Physikalisches Institut, Ruprecht-Karls-Universität Heidelberg, Heidelberg, Germany
- ¹³ School of Physics, University College Dublin, Dublin, Ireland
- ¹⁴ Sezione INFN di Bari, Bari, Italy
- ¹⁵ Sezione INFN di Bologna, Bologna, Italy
- ¹⁶ Sezione INFN di Cagliari, Cagliari, Italy
- ¹⁷ Università e INFN, Ferrara, Ferrara, Italy
- ¹⁸ Sezione INFN di Firenze, Firenze, Italy
- ¹⁹ Laboratori Nazionali dell'INFN di Frascati, Frascati, Italy
- ²⁰ Sezione INFN di Genova, Genova, Italy
- ²¹ Università & INFN, Milano-Bicocca, Milano, Italy
- ²² Sezione di Milano, Milano, Italy
- ²³ Sezione INFN di Padova, Padova, Italy
- ²⁴ Sezione INFN di Pisa, Pisa, Italy
- ²⁵ Sezione INFN di Roma Tor Vergata, Roma, Italy
- ²⁶ Sezione INFN di Roma La Sapienza, Roma, Italy
- ²⁷ Henryk Niewodniczanski Institute of Nuclear Physics Polish Academy of Sciences, Kraków, Poland
- ²⁸ AGH - University of Science and Technology, Faculty of Physics and Applied Computer Science, Kraków, Poland
- ²⁹ National Center for Nuclear Research (NCBJ), Warsaw, Poland
- ³⁰ Horia Hulubei National Institute of Physics and Nuclear Engineering, Bucharest-Magurele, Romania
- ³¹ Petersburg Nuclear Physics Institute (PNPI), Gatchina, Russia
- ³² Institute of Theoretical and Experimental Physics (ITEP), Moscow, Russia
- ³³ Institute of Nuclear Physics, Moscow State University (SINP MSU), Moscow, Russia
- ³⁴ Institute for Nuclear Research of the Russian Academy of Sciences (INR RAN), Moscow, Russia
- ³⁵ Yandex School of Data Analysis, Moscow, Russia
- ³⁶ Budker Institute of Nuclear Physics (SB RAS), Novosibirsk, Russia
- ³⁷ Institute for High Energy Physics (IHEP), Protvino, Russia
- ³⁸ ICCUB, Universitat de Barcelona, Barcelona, Spain
- ³⁹ Universidad de Santiago de Compostela, Santiago de Compostela, Spain
- ⁴⁰ European Organization for Nuclear Research (CERN), Geneva, Switzerland
- ⁴¹ Institute of Physics, Ecole Polytechnique Fédérale de Lausanne (EPFL), Lausanne, Switzerland
- ⁴² Physik-Institut, Universität Zürich, Zürich, Switzerland
- ⁴³ Nikhef National Institute for Subatomic Physics, Amsterdam, The Netherlands
- ⁴⁴ Nikhef National Institute for Subatomic Physics and VU University Amsterdam, Amsterdam, The Netherlands
- ⁴⁵ NSC Kharkiv Institute of Physics and Technology (NSC KIPT), Kharkiv, Ukraine
- ⁴⁶ Institute for Nuclear Research of the National Academy of Sciences (KINR), Kyiv, Ukraine
- ⁴⁷ University of Birmingham, Birmingham, U.K.
- ⁴⁸ H.H. Wills Physics Laboratory, University of Bristol, Bristol, U.K.
- ⁴⁹ Cavendish Laboratory, University of Cambridge, Cambridge, U.K.
- ⁵⁰ Department of Physics, University of Warwick, Coventry, U.K.
- ⁵¹ STFC Rutherford Appleton Laboratory, Didcot, U.K.
- ⁵² School of Physics and Astronomy, University of Edinburgh, Edinburgh, U.K.
- ⁵³ School of Physics and Astronomy, University of Glasgow, Glasgow, U.K.
- ⁵⁴ Oliver Lodge Laboratory, University of Liverpool, Liverpool, U.K.
- ⁵⁵ Imperial College London, London, U.K.
- ⁵⁶ School of Physics and Astronomy, University of Manchester, Manchester, U.K.

- ⁵⁷ *Department of Physics, University of Oxford, Oxford, U.K.*
- ⁵⁸ *Massachusetts Institute of Technology, Cambridge, MA, U.S.A.*
- ⁵⁹ *University of Cincinnati, Cincinnati, OH, U.S.A.*
- ⁶⁰ *University of Maryland, College Park, MD, U.S.A.*
- ⁶¹ *Syracuse University, Syracuse, NY, U.S.A.*
- ⁶² *Pontifícia Universidade Católica do Rio de Janeiro (PUC-Rio), Rio de Janeiro, Brazil, associated to ²*
- ⁶³ *University of Chinese Academy of Sciences, Beijing, China, associated to ³*
- ⁶⁴ *School of Physics and Technology, Wuhan University, Wuhan, China, associated to ³*
- ⁶⁵ *Institute of Particle Physics, Central China Normal University, Wuhan, Hubei, China, associated to ³*
- ⁶⁶ *Departamento de Física, Universidad Nacional de Colombia, Bogota, Colombia, associated to ⁸*
- ⁶⁷ *Institut für Physik, Universität Rostock, Rostock, Germany, associated to ¹²*
- ⁶⁸ *National Research Centre Kurchatov Institute, Moscow, Russia, associated to ³²*
- ⁶⁹ *National Research Tomsk Polytechnic University, Tomsk, Russia, associated to ³²*
- ⁷⁰ *Instituto de Física Corpuscular, Centro Mixto Universidad de Valencia - CSIC, Valencia, Spain, associated to ³⁸*
- ⁷¹ *Van Swinderen Institute, University of Groningen, Groningen, The Netherlands, associated to ⁴³*
- ^a *Universidade Federal do Triângulo Mineiro (UFTM), Uberaba-MG, Brazil*
- ^b *Laboratoire Leprince-Ringuet, Palaiseau, France*
- ^c *P.N. Lebedev Physical Institute, Russian Academy of Science (LPI RAS), Moscow, Russia*
- ^d *Università di Bari, Bari, Italy*
- ^e *Università di Bologna, Bologna, Italy*
- ^f *Università di Cagliari, Cagliari, Italy*
- ^g *Università di Ferrara, Ferrara, Italy*
- ^h *Università di Genova, Genova, Italy*
- ⁱ *Università di Milano Bicocca, Milano, Italy*
- ^j *Università di Roma Tor Vergata, Roma, Italy*
- ^k *Università di Roma La Sapienza, Roma, Italy*
- ^l *AGH - University of Science and Technology, Faculty of Computer Science, Electronics and Telecommunications, Kraków, Poland*
- ^m *LIFAELS, La Salle, Universitat Ramon Llull, Barcelona, Spain*
- ⁿ *Hanoi University of Science, Hanoi, Viet Nam*
- ^o *Università di Padova, Padova, Italy*
- ^p *Università di Pisa, Pisa, Italy*
- ^q *Università degli Studi di Milano, Milano, Italy*
- ^r *Università di Urbino, Urbino, Italy*
- ^s *Università della Basilicata, Potenza, Italy*
- ^t *Scuola Normale Superiore, Pisa, Italy*
- ^u *Università di Modena e Reggio Emilia, Modena, Italy*
- ^v *Iligan Institute of Technology (IIT), Iligan, Philippines*
- ^w *Novosibirsk State University, Novosibirsk, Russia*
- [†] *Deceased*